PHENOMENA IN PENETRATING PIERCING BULLETS IN ARMORED STEEL PLATE

The presented work studied the response of new generation armored steel plates PROTAC 500 to the ballistic testing with armored piercing bullets with a core of tungsten carbide, charge 7,62 mm, and interactions between the piercing bullets and the armored steel plate were also investigated. The most obvious and significant phenomena in penetrating of the piercing bullets Nammo AP8 in steel target PROTAC 500 are strain hardening of steels, the appearance of cracks and local failure, adiabatic shear bands (ASB) with related phase transformations, and melting as well as alloying at the border of the bullet / the steel plate.

Key words: armored steel, plate, mechanical properties, ballistic testing, bullet, adiabatic shear band

INTRODUCTION

The selection of the appropriate armored material is crucial to ensure the adequate safety and mobility transport systems [1]. When selecting or developing the appropriate materials for the armor it is necessary to achieve the best possible compromise between the required mechanical properties of materials, minimizing the density and the final price of the product [2]. With the appropriate production technology, which includes synthesis, hot forming, heat treatment, etc. [3]. High strength low alloy steel of good functional properties at affordable prices can be produced [4]. By improving the strength and toughness of the steel the required thickness and the weight of the steel shell is reduced [5]. Such steels are competitive to other materials for the armor [6]. In the context of this study, we carried out a ballistic test of high strength low alloy steel PROTAC 500, whose mechanical properties and testing conditions are collected in Table 1.

Steel PROTAC 500 belongs to the group of high strength low alloy (HSLA) steels. It is made in Slovenian steelwork ACRONI by the standard industrial procedures, and the relevant mechanical properties are achieved by quenching and tempering.

Preliminary tests of the mechanical properties of the steel have indicated the possibility of using steel PROTAC 500 for light armored vehicles. Ballistic testing was performed by using 7,62 mm armoured piercing bullets of the Swedish manufacturer Nammo (German

J. Bernetič, B. Kosec, A. Nagode, B. Karpe, L. Kosec, Faculty of Natural Sciences and Engineering, University of Ljubljana, Ljubljana, Slovenia. G. Kosec, B. Podlipec, S. Kanalec, ACRONI d.o.o., Jesenice, Slovenia, Z. Burzic, MTI, Belgrade, Serbia. F. Vodopivec, IMT, Ljubljana, Slovenia

Table 1 **Mechanical properties of steel PROTAC 500**

Testing temperature /°C	- 40
Yeald strength $R_{P0,2}$ /MPa	1 200
Tensile strength R_m /MPa	1 600
Elongation A_5 /%	8
Impact toughness / J	20
Hardness / HB	480 – 530

standard VPAM, level 11, and the American standard STANAG 4569, Level 3), to examine the interaction between a bullet and a steel plate [7]. Armored piercing bullets, containing the rigid core (generally of high strength steel), which results in the conversion of the total kinetic energy of the bullets to the deformation of the target. The peculiarity of this bullet is the core of tungsten carbide (WC - Co) [8].

When the bullet hits its target, first the formation of pressure waves (cyclic stress) are formed, that spread through the target material and shall be deducted from the back side of the target as tensile waves. These waves reinforce the material, at a certain intensity of interaction between the waves of pressure or tension and can lead to the formation of adiabatic shear bands, cracks and crack growth. The material resistance to compressive and tensile waves is improved by increasing the strength and toughness.

The deformation mechanisms at low strain rate are relatively homogeneous, while at extremely high speeds they are more complex. Here it comes to the extreme strain localization in narrow bands called adiabatic shear bands (ASB) [9,10]. The belt is during the deformation very hot, whereby there a transformation of the austenite phase originates, after the load it is rapidly cooled, which results in the transformation to martensite, and thus a high hardness and brittleness of the

steel in the ASB occurs. The shear zones are therefore weak areas in the steel.

EXPERIMENTAL WORK

For the ballistics testing a steel PROTAC 500 testing plate with dimensions of 500 x 500 x 20,8 mm was used. Six shots were conducted under the terms of the standard VPAM and STANAG 4569 (Table 2) [11,12].

Nammo AP8 is the cartridge of an armored-penetrating bullet caliber 7,62 x 51 mm (,308 Winchester) [11]. American label of the cartridge is the M993. It tends to be used against targets with light armor. Bullet is capable of destroying such targets by 2 to 3 times the distance from the armored piercing of bullets with steel cores. The bullet is made up of a core of tungsten carbide, mounted in an aluminium cup shell is made of steel coated with brass.

Table 2 **Terms of ballistic test according to the standard VPAM and STANAG 4569**

Producer	Nammo AP8
Standard	VPAM – level 11
Caliber	,308 Win
Cartridge	FMJ/PB/WC
Bullet mass /g	8,4 ± 0,1
Bullet speed /m/s	930 ± 10
Distance from target /m	10 ± 0,5
Bullet energy /J	3 633

After the ballistics test was excluded from the testing panel three testing samples were cut. The first sample was then cut in several planes perpendicular to the direction of the shot, the other two samples were cut through the penetration of bullets in a plane parallel to the direction of the shot [13]. For the surface metallographic analysis samples were etched with an aqueous solution of ferric chloride. Prepared in this way the surface were examined by metallographic investigation methods. Analysis of macro and microstructure were performed on an optical microscope Olympus BX61. We were interested in particular areas with a different microstructure of the base and the places where the cracks and adiabatic shear bands (ASP) are found. This was followed by analysis with the scanning electron microscope (SEM) JEOL 5610, which allows the observation of microstructure and qualitative and quantitative chemical analysis [14]. The images were recorded at various magnifications, especially the areas where had been ASB, cracks, pores, and where they were traces of melting and mixing of materials.

Hardening of the steel plate after penetrating piercing bullets was determined by measuring the Vickers hardness (HV). The fractographic analysis of cracks that have occurred during the ballistic test, for which it was necessary to break down the samples have been done. To determine the mechanism of formation and spreading of the cracks and localized the nature of the fractured surfaces were ignoring and destroying extracts of the errors and faults at liquid nitrogen temperature.

RESULTS AND DISCUSSION

In Figure 1 there is the microstructure of the steel PROTAC 500 before the ballistic test. The microstructure consists of tempered martensite, and the hardness of such steel is 540 HV.
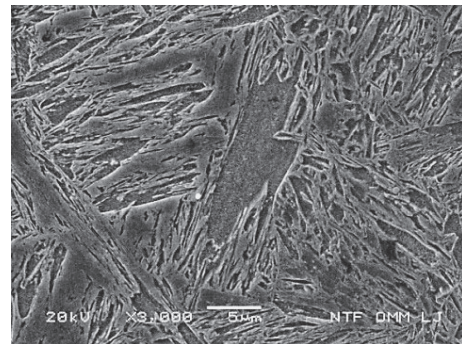

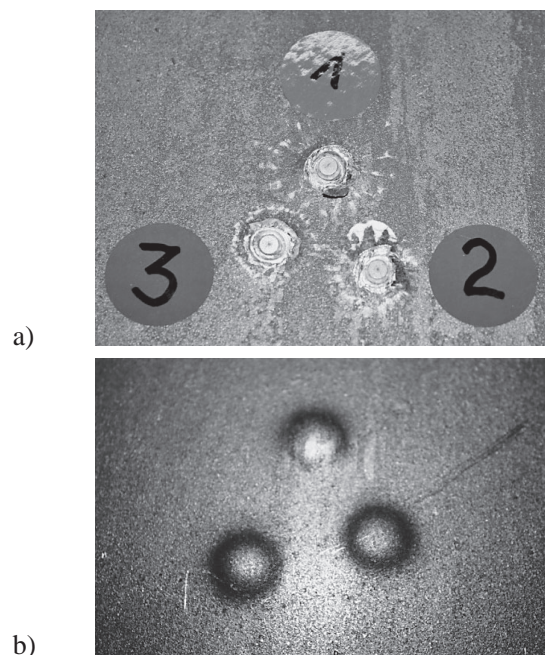**Figure 1** The microstructure of steel PROTAC 500 (SEM)

a)

b)

Figure 2 Front (a) and back (b) side of the steel plate PROTAC 500 after ballistic testing – details of three shots

In Figure 2 (a) there is a front side of the panels PROTAC 500 after ballistics testing with the markings of three samples were have cut and prepared for further analysis. All armored piercing bullets are stopped in the plate. In interpreting the results of ballistic tests is the most important imformation if a bullet penetrates the target [15]. In Figure 2 (below) there is the back side of the panel after ballistic test. In none of the shots no perforation of the panel occurred. The testing results and descriptions of the standard VPAM are in Table 3.

Table 3 **Parameters of the ballistic tests and description of the results**

	Sample 1	Sample 2	Sample 3
Distance /m	10	10	10
Shot angle /°	90	90	90
Impact velocity /m/s	929	931	937
Bullet energy /J	3 624,77	3 640,40	3 687,47
Break trough	No	No	No

By the shot to the sample 1 the bulge with a crack was formed, that does not transmit light by other shots, but it was smaller bulge without cracks. For a more detailed picture of the interactions between bullets and plate the samples for metallographic analysis were prepared.
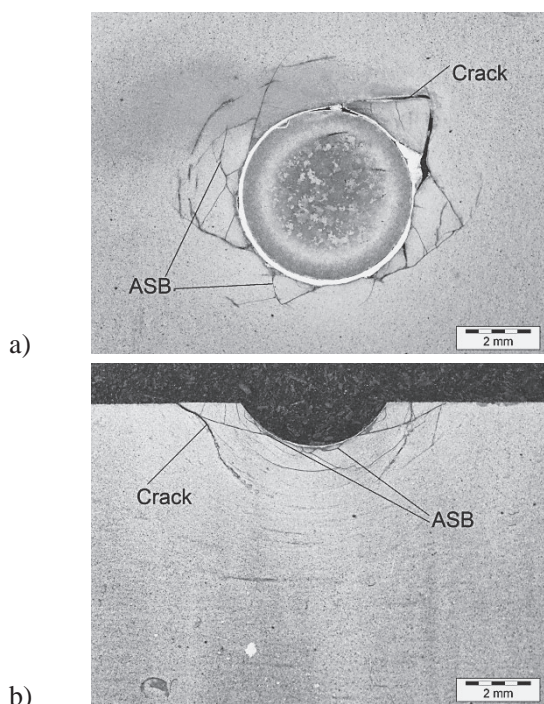

Figure 3 Macroscopic cross-sectional images of the sample 1 (a - upper level, b - lower level)

Figure 3 consists of a macro-picture of two analytical levels of sample 1 cross-sections. In Figure 3a there is a cross-sectional view of the upper level of the sample, where there are a significant number of cracks, and branched adiabatic shear bands which extend from the border between the envelope bullets (bright narrow band around the circumference of the core) and the base material towards the interior of the target. In Figure 3b is a half cross-sectional view of the lower level of the sample. At this level it is less ASB and cracks and at the same time do not go so far into the interior of the target. Most of the kinetic energy of the projectile to the lower level is already spent.

Figure 4 shows the macro-picture breakthroughs balls on the analysis of samples 2 and 3, giving examples of cracks and ASB. In the area between the ball and the lower edge of the steel plate they have cracks in the form of a pin. Breakthrough with pin is a common
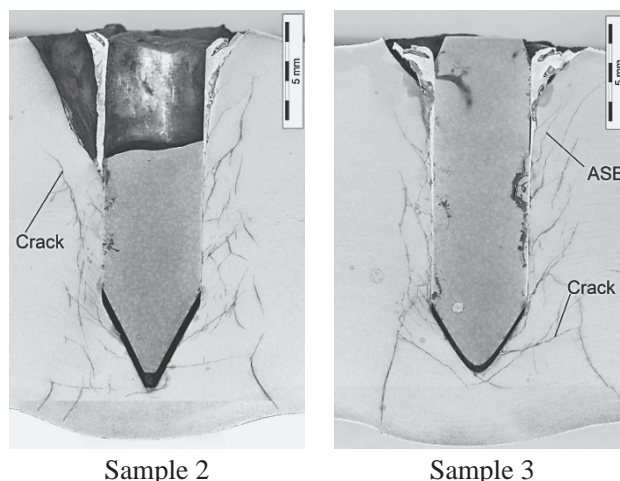

Sample 2   Sample 3

Figure 4 Macroscopic picture of breakthroughs bullets trough the samples 2 and 3, marked as cracks and ASB

mechanism of penetration through the high strength steels in which the phenomenon of ASB has an important role. The formation of the plug occurs when the thickness of the target is approaching to the diameter of the bullet. Notice also that the bullet after a stoppage due to elastic deformation and the target are slightly separated. For the sample 3 we have also measured the length of the cracks and ASB. The average length of the cracks on the sample 3 is 3,9 mm, the average length of the ASB was 4,3 mm, which indicates a very high-speed deformation. In figure 5 is transformed ASB, which extends from the edge of penetration (primary ASB) inside the plate (secondary ASB), the medium level of sample 1 ASB in the investigated steel vary in length, width and branching. Mechanism for the growth and spread of ASB is not a generally accepted criteria, in the literature is generally assumed that the spread and growth of ASB are related dictated to the dynamic recrystallization inside the ASB [12].
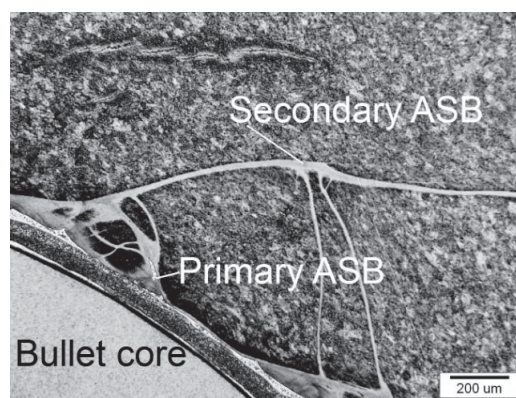

Figure 5 The microstructure of the cross-section of the target at the centre of the bullet. Course of ASB and cracks (sample 1)

In Figure 6 the distribution of hardness of the steel in the vicinity of the bullet's penetration and bullet cores (gray scale) to the sample 3 is the result of 855 measurements in a mutual distance of 400 mm. Hardness distribution map shows the progress and scope of consolida-

tion deformation of the steel in the vicinity of the projectile penetration. The maximum difference between the average hardness of the undeformed and deformed steel hardness is 95 HV on a sample 3. For the samples 3 and 2 we performed the measurements of the hardness of ASB. On the sample 3 was performed 32 and on a sample of 2 13 hardness measurements of ASB. Hardness of the steel in the ASB was significantly higher than the initial hardness of steel. Maximum hardness of 775 HV was measured in the ASB on the sample 3. The hardness of the steel in the ASB is about 170 HV is higher than the initial hardness of the steel (sample 3), on the sample 2 is higher for about 160 HV.
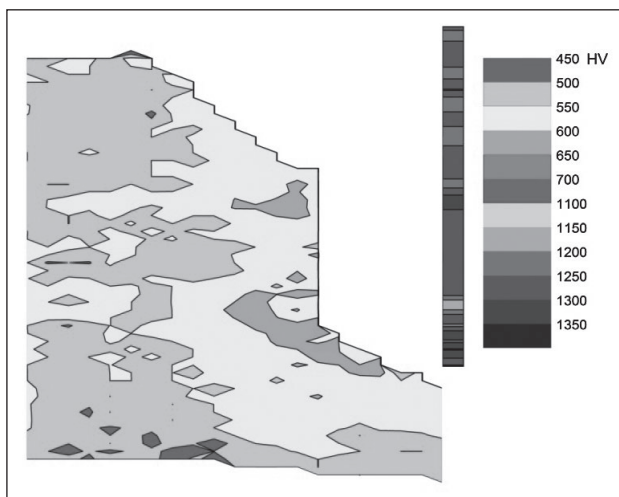

Figure 6 Distribution of hardness of the steel in the vicinity of the bullet penetration through sample 3

CONCLUSIONS

The research analyzed the ballistic properties of armor steel plate PROTAC 500 against armored piercing bullets caliber 7,62 mm.

The most obvious and significant phenomena in penetrating of the piercing bullets Nammo AP8 in steel target (plate) PROTAC 500 are:
- strain hardening of steels,
- the appearance of cracks and local failure,
- adiabatic shear bands (ASP) and related phase transformations: austenitic, martensitic, melting, solidification, and

- melting and alloying at the border of the bullet / the steel of the target (plate).

Acknowledgement

REFERENCES

[1]   C. J. Hu, P. W. Lee, Journal of the Chinese Institute of Engineers 25 (2002) 1, 99-107.
[2]   S. Baloš, V. Grabulov, L. Sidjanin, M. Pantić, Materials and Design 31(2010) 2916-2924.
[3]   A. Bakkaloglu, Materials Letters 56 (2002) 200-209.
[4]   J. Trajkovski, R. Kunc, V. Pepel, I. Prebil, Materials and Design, 66 (2015), 37-45.
[5]   J. Bernetič, B. Bradaškja, G. Kosec, E. Bricelj, B. Kosec, F. Vodopivec, L. Kosec, Metalurgija 49 (2010) 1, 29-32.
[6]   M. A. Iqbal, K. Sentil, P. Bhargava, N. K. Gupta, International Journal of Impact Engineering 78 (2015), 98-111.
[7]   T. Demir, M. Übeyli, R. O. Yildrim, Materials and Design 29 (2008) 10, 2009-2016.
[8]   H. S. Atapek, Defence Science Journal 61 (2011), 81-87.
[9]   Z. Q. Duan, S.X. Li, D.W. Huang, Fatigue & Fracture of Engineering Materials & Structures 26 (2003) 12, 1119-1126.
[10] S. Dey, T. Børvik, O. S. Hopperstadt, J. R. Leinum, M. Langseth, International Journal of Impact Engineering 33 (2004), 1005-1038.
[11] Y. Bai, B. Dodd, Adiabatic Shear Localization: Occurrence, Theories, and Applications, Pergamon Press, 1992.
[12] NATO standard - STANAG 4569. Protection levels for Occupants af Logistic and Light Armoured Vehicles, NATO AEP-55, 2013.
[13] N. Kilic, S. Bedir, A. Erdik, B. Ekici, A. Tasdemirici, M. Guden, Materials and Design 63 (2014), 427-438.
[14] G. Kosec, A. Nagode, I. Budak, A. Antic, B. Kosec, Engineering Failure Analysis 18 (2011) 1, 450-454.
[15] T. Børvik, S. Dey, A. H. Clausen, International Journal of Impact Engineering 36 (2009) 7, 948-964.